The KD_2PO_4 ferroelectrics in external fields conjugate to the order parameter: Shear stress σ_6

I. V. Stasyuk,[1] R. R. Levitskii,[1] I. R. Zachek,[2] and A. P. Moina[1,*]

[1]*Institute for Condensed Matter Physics, 1 Svientsitskii Street, UA-79011, Lviv, Ukraine*
[2]*State University ''Lviv Polytechnics,'' 12 Bandery Street, UA-79013, Lviv, Ukraine*

(Received 15 February 2000)

A microscopic model of the influence of the conjugate to the order parameter external fields—electric field E_3 and shear stress σ_6—on deuterated KD_2PO_4-type ferroelectrics is presented. The major mechanisms for this influence are the splitting of the Slater-Takagi energies of the short-range correlations and the effective field created by piezoelectric coupling with shear strain ε_6. The T_C vs σ_6 phase diagram of KD_2PO_4 is constructed, and the stress dependences of the dielectric, piezoelectric, and elastic characteristics associated with strain ε_6 are discussed.

Hydrostatic pressure studies[1] have proven to be extremely useful in elucidating the role of the hydrogen subsystem in the phase transition and dielectric response of the KH_2PO_4-family crystals. They revealed[2,3] a strong dependence of the transition temperature and dielectric characteristics of these crystals on the geometry of hydrogen bonds (in particular, on the separation between the two equilibrium hydrogen sites on a bond).

Along with the shift of hydrogens at ordering, other changes in the geometry of the crystals, accompanying their polarization (at the phase transition or in response to the electric field) can be equally important. For instance, a distortion of PO_4 groups takes place at the transition, so that the P ions move closer to the upper (or lower, depending on the polarization direction) oxygen ions, and the lines connecting upper and lower oxygens of each PO_4 group stop being perpendicular.[4] Also, one of the diagonals of the square-shaped projection of the tetragonal unit cell on the ab plane elongates, while the other shortens, turning this square into a rhomb (the angle between the corresponding sides of the square and of the rhomb defines the shear strain ε_6). Thereby, the angle between hydrogen bonds along the adjacent square (rhomb) sides deviates from $\pi/2$.

A natural way to explore the role of structural changes occurring in the crystals at the phase transition is to study behavior of the crystals in external fields that would induce identical changes. For the KH_2PO_4-family ferroelectrics, such fields are the shear stress σ_6 and the electric field E_3 applied along the ferroelectric axis c. Via the piezoelectric effect, both of them induce polarization P_3 and strain ε_6; polarization and strain of the same symmetry arise spontaneously in the low-temperature phase.

The way the fields conjugate to the order parameter affect the phase transition in the system is already clear from the analysis of the Landau expansion for thermodynamic potential

$$G = G_0 + \frac{\tilde{a}'}{2}(T-T_0)\xi^2 + \frac{\tilde{b}}{4}\xi^4 + \frac{\tilde{c}}{6}\xi^6 - \tilde{E}\xi$$

($\tilde{a}'>0$, $\tilde{b}<0$; for KD_2PO_4 ξ is a certain linear combination of polarization P_3 and strain ε_6, and $\tilde{E}$ is a linear combina-

tion of E_3 and σ_6). In a linear in $\tilde{E}$ approximation, the temperature of the first order phase transition increases with $\tilde{E}$ as

$$T_C = T_{C0} - \tilde{E}\frac{12\tilde{c}}{7\tilde{a}'\tilde{b}}\sqrt{\frac{4\tilde{c}}{-3\tilde{b}}},$$

and the phase equilibrium curves terminate at the critical points ($\pm\tilde{E}^*, T^*$)

$$\tilde{E}^* = \frac{8}{15}\tilde{a}\sqrt{\frac{-3\tilde{b}}{10\tilde{c}}},$$

$$T^* = T_{C0} + \frac{7}{5}\frac{3\tilde{b}^2}{16\tilde{c}\tilde{a}'}.$$

A microscopic theory of these phenomena and accompanying them changes in the physical properties of the KD_2PO_4-type systems is still absent. Such a theory must take into account the facts, that the mentioned above changes in the crystal structure affect the short-range correlations between hydrogens, and that piezoelectric coupling with shear strain ε_6 produces long-range molecular fields[5] analogous to the external electric field E_3.

In the calculations of the static properties of the KH_2PO_4-family crystals performed within the pseudospin proton ordering model, effects related to spontaneous strain ε_6 are usually neglected. Studying the influence of the fields σ_6 and E_3 we *en route* take these effects into account and obtain a more consistent description of KD_2PO_4 in the ferroelectric phase. We also can calculate the elastic and piezoelectric characteristics of the crystals and find out to what extent the peculiarities of their temperature behavior can be attributed to the hydrogen subsystem.

These studies provide helpful information about the theory of mixed $Rb_{1-x}(NH_4)_xH_2PO_4$-type systems. Thus, we estimate a magnitude of the piezoelectric coupling which gives rise to random electric fields in such systems,[6] smearing out the transition between the spin-glass phase—paraelectric phase.[7] Also we elucidate the changes in the energies of deuteron configurations induced by the strain ε_6. These changes can be a source of randomness in the short-

range interactions in these systems, though not as important as extra hydrogen bonding brought by impurity ammonium ions.

In the present paper we propose a generalization of the conventional proton ordering model that takes into account effects of the shear strain ε_6: piezoelectric fields and splitting of the short-range Slater-Takagi energy levels. We verify that the developed model can describe the temperature peculiarities of associated with the strain ε_6 elastic and piezoelectric characteristics of the crystal at atmospheric pressure. Influence of the stress σ_6 on the phase transition, dielectric, elastic, and piezoelectric properties of deuterated KD$_2$PO$_4$ is investigated. The T_C-σ_6 phase diagram is constructed and calculated dependences of the physical characteristics on stress σ_6 are presented.

I. THE MODEL

We consider a deuterated crystal of the KD$_2$PO$_4$ type to which external electric field E_3 and shear stress σ_6 are applied. Both E_3 and σ_6 induce polarization P_3 and strain ε_6 in the crystal; polarization and strain of the same type arise spontaneously in the ordered phase.

The entire Hamiltonian of the model consists of a ''seed'' part, independent of deuteron subsystem configuration and attributed to a host lattice of heavy ions, and of a pseudospin Hamiltonian of the deuteron subsystem, including short-range and long-range counterparts

$$H = NU_{\text{seed}} + H_{\text{long}} + H_{\text{short}} - \sum_{qf} \mu_3 E_3 \frac{\sigma_{qf}}{2}, \qquad (1)$$

N is the number of primitive cells; tunneling is neglected. The last term in the Hamiltonian describes interaction of the longitudinal effective dipole moments of primitive cells μ_3 with external electric field applied along the ferroelectric axis c. The dipole moments are created by heavy ions polarization and displacements, triggered by deuteron ordering.

The ''seed'' energy expressed in terms of the electric field E_3 and strain ε_6 has the standard form[8]

$$U_{\text{seed}} = \frac{\bar{v}}{2} c_{66}^{E0} \varepsilon_6^2 - \bar{v} e_{36}^0 E_3 \varepsilon_6 - \frac{\bar{v}}{2} \chi_{33}^0 E_3^2 \qquad (2)$$

and includes the elastic, piezoelectric, and electric counterparts, which do not depend on hydrogen arrangement. c_{66}^{E0}, e_{36}^0, and χ_{33}^0 are the so-called ''seed'' elastic constant, coefficient of the piezoelectric stress, and dielectric susceptibility, respectively; $\bar{v} = v/k_B$, v is the primitive cell volume; k_B is the Boltzmann constant.

H_{long} is the Hamiltonian of the long-range interactions between deuterons (dipole-dipole and lattice mediated[9]) taken into account in the mean field approximation. In addition, piezoelectric coupling induces additional molecular field[5] linear in strain ε_6. Hence

$$H_{\text{long}} = \frac{1}{2} \sum_{q'f'qf} J_{ff'}(qq') \frac{\langle \sigma_{qf} \rangle}{2} \frac{\langle \sigma_{q'f'} \rangle}{2}$$

$$- \sum_{qf} \left[\left(\sum_{q'f'} J_{ff'}(qq') \frac{\langle \sigma_{q'f'} \rangle}{2} \right) \frac{\sigma_{qf}}{2} - 2\psi_6 \varepsilon_6 \frac{\sigma_{qf}}{2} \right]$$

$$= 2N\nu\eta^2 - \sum_{qf} (2\nu\eta - 2\psi_6\varepsilon_6) \frac{\sigma_{qf}}{2}, \qquad (3)$$

where

$$4\nu = J_{11} + 2J_{12} + J_{13}$$

is the eigenvalue of the long-range interaction matrix Fourier transform $J_{ff'} = \Sigma_{\mathbf{R}_q - \mathbf{R}_{q'}} J_{ff'}(qq')$;

$$\eta = \langle \sigma_{q1} \rangle = \langle \sigma_{q2} \rangle = \langle \sigma_{q3} \rangle = \langle \sigma_{q4} \rangle$$

is the mean value of the Ising pseudospin $\sigma_{qf} = \pm 1$ whose two eigenvalues are assigned to two equilibrium positions of a deuteron on the fth bond in the qth primitive cell. As one can see, the piezoelectric field $\psi_6 \varepsilon_6$ is analogous to external electric field E_3. Under hydrostatic pressure, the corresponding fields $\Sigma_{i=1}^3 \psi_{ci}\varepsilon_i \eta$ are proportional to the diagonal components of lattice strain tensor and to the mean values of pseudospins;[3,5] therefore, they are analogous to internal molecular fields created by the long-range deuteron-deuteron interactions.

Let us consider now the Hamiltonian of the short-range configurational interactions between deuterons. A proper approximation is the four-particle cluster approximation,[9] which adequately takes into account the geometry of these interactions.
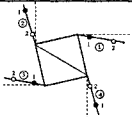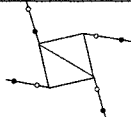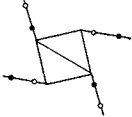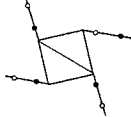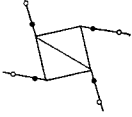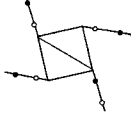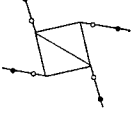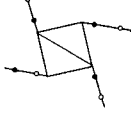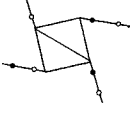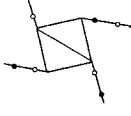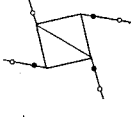
The Hamiltonian is usually chosen such as to reproduce the energy levels of the Slater-type model for KDP (see, for instance, Ref. 10)—the Slater energies ε, w, and w_1 ($\varepsilon \ll w \ll w_1$), determined by the energies of up-down ε_s, lateral ε_a, single-ionized ε_1, and double-ionized ε_0 deuteron configurations

$$\varepsilon = \varepsilon_a - \varepsilon_s, \quad w = \varepsilon_1 - \varepsilon_s, \quad w_1 = \varepsilon_0 - \varepsilon_s.$$

If $\varepsilon_6 = 0$, the ''up'' and ''down'' deuteron configurations have the same energy ε_s, assumed to be the lowest. (The ''up'' configuration is the one with two hydrogens in potential wells being close to upper oxygens of a given PO$_4$ group, while the hydrogens on the two other bonds are close to the neighboring tetrahedra.) Correspondingly, lateral configurations with two hydrogens close to an upper and a lower oxygens are fourfold degenerate; single-ionized configurations with only one (or three) hydrogens close to a given group are eightfold degenerate, and double-ionized configurations with four (or zero) hydrogens are twice degenerate.
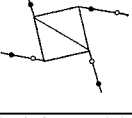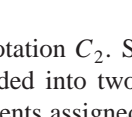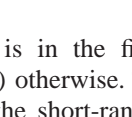
The strain ε_6 splits certain energy levels of the conventional Slater-Takagi model (see Table I). Since the system is no longer symmetric with respect to a mirror rotation S_4 (the operation changes the sign of polarization and strain ε_6), the energy of up-down configurations ($i=1,2$) splits to two different levels, and the energy level of lateral configurations splits to two twice degenerate levels ($i=5,6$) and ($i=7,8$). Configurations corresponding to each level are symmetric

TABLE I. Deuteron configurations and their energies with the splitting due to strain ε_6 taken into account.

i	$\sigma_1\sigma_2\sigma_3\sigma_4$	E_i	i	$\sigma_1\sigma_2\sigma_3\sigma_4$	E_i
1	$+ + + +$	$\varepsilon_s - \delta_{s6}\varepsilon_6$	9	$- - - +$	$\varepsilon_1 - \delta_{16}\varepsilon_6$
2	$- - - -$	$\varepsilon_s + \delta_{s6}\varepsilon_6$	10	$- - + -$	
3	$+ - + -$	ε_0	11	$- + - -$	
4	$- + - +$	ε_0	12	$+ - - -$	
5	$+ + - -$	$\varepsilon_a + \delta_{a6}\varepsilon_6$	13	$+ + - +$	$\varepsilon_1 + \delta_{16}\varepsilon_6$
6	$- - + +$	$\varepsilon_a + \delta_{a6}\varepsilon_6$	14	$+ + + -$	
7	$- + + -$	$\varepsilon_a - \delta_{a6}\varepsilon_6$	15	$- + + +$	
8	$+ - - +$	$\varepsilon_a - \delta_{a6}\varepsilon_6$	16	$+ - + +$	

with respect to π rotation C_2. Similarly, single-ionized configurations are divided into two groups, with the c component of dipole moments assigned to each configuration being directed up ($i = 9,10,11,12$) or down ($i = 13,14,15,16$).

In the hydrostatic pressure case, the changes in the Slater energies are usually attributed to pressure-induced changes in the D-site distance δ.[3,11] Here we assume that δ does not depend on strain ε_6. Instead, the energies of deuteron configurations are altered only by splitting of the degenerated levels due to lowering of the system symmetry. From geometric point of view, this happens mostly because the PO$_4$ groups are distorted (the P ions shift up or down) and the angle between perpendicular in the paraelectric phase hydrogen bonds is changed. All splittings are taken as linear functions of strain ε_6.

To rewrite the energies of deuteron configurations E_i in terms of pseudospins, we associate the configuration operator $\hat{N}_i$ with the configuration i according to the following rule: each operator is a product of four factors, one per each hydrogen bond, each factor being equal to $\frac{1}{2}(1 + \sigma_{qf})$ if deu-

teron is in the first minimum at the fth bond and $\frac{1}{2}(1 - \sigma_{qf})$ otherwise. Then the entire Hamiltonian of the system, with the short-range interactions taken into account within the four-particle cluster approximation, takes the form

$$\hat{H}^{(4)} = N(U_{\text{seed}} + 2\nu\eta^2) + \sum_q \hat{H}_q^{(4)},$$

$$\hat{H}_q^{(4)} = -\sum_{f=1}^{4} \frac{z}{\beta} \frac{\sigma_{qf}}{2} + \frac{\varepsilon_6}{4}(-\delta_{s6} + 2\delta_{16})\sum_{f=1}^{4} \frac{\sigma_{qf}}{2}$$

$$-\varepsilon_6(\delta_{s6} + 2\delta_{16})\left[\frac{\sigma_{q1}}{2}\frac{\sigma_{q2}}{2}\frac{\sigma_{q3}}{2} + \frac{\sigma_{q1}}{2}\frac{\sigma_{q2}}{2}\frac{\sigma_{q4}}{2}\right.$$

$$\left. + \frac{\sigma_{q1}}{2}\frac{\sigma_{q3}}{2}\frac{\sigma_{q4}}{2} + \frac{\sigma_{q2}}{2}\frac{\sigma_{q3}}{2}\frac{\sigma_{q4}}{2}\right]$$

$$+ (V + \delta_{a6}\varepsilon_6)\left[\frac{\sigma_{q1}}{2}\frac{\sigma_{q2}}{2} + \frac{\sigma_{q3}}{2}\frac{\sigma_{q4}}{2}\right]$$

$$+(V-\delta_{a6}\varepsilon_6)\left[\frac{\sigma_{q2}}{2}\frac{\sigma_{q3}}{2}+\frac{\sigma_{q4}}{2}\frac{\sigma_{q1}}{2}\right]$$

$$+U\left[\frac{\sigma_{q1}}{2}\frac{\sigma_{q3}}{2}+\frac{\sigma_{q2}}{2}\frac{\sigma_{q4}}{2}\right]$$

$$+\Phi\frac{\sigma_{q1}}{2}\frac{\sigma_{q2}}{2}\frac{\sigma_{q3}}{2}\frac{\sigma_{q4}}{2}. \tag{4}$$

When strain ε_6 is not taken into account, the short-range part of the Hamiltonian is symmetric with respect to a simultaneous change of signs of all pseudospins and, hence, contains only two- and four-particle terms. However, due to the splitting of up-down and single-ionized configurations there arise terms odd in pseudospins (one- and three-particle), whose prefactors are, naturally, proportional to the strain ε_6 and to the constants of the splitting δ_{s6} and δ_{16}.

In Eq. (4) the following notations are used:

$$V=-\frac{1}{2}w_1,\quad U=\frac{1}{2}w_1-\varepsilon,\quad \Phi=4\varepsilon+2w_1-8w,$$

and

$$z=\beta[-\Delta+2\nu\eta-2\psi_6\varepsilon_6+\mu_3E_3].$$

The short-range interactions with the sites neighboring to the qfth site, which are not explicitly included into the four-particle cluster Hamiltonian, are taken into account via the cluster field Δ.

Using the condition of equality of the mean values of pseudospins calculated with the four-particle (4) and single-particle deuteron Hamiltonians

$$\hat{H}_{qf}=-\frac{z-\beta\Delta}{\beta}\frac{\sigma_{qf}}{2},$$

we exclude the parameter Δ and obtain

$$\eta=\frac{m}{D}, \tag{5}$$

where

$$m=\sinh(2z+\beta\delta_{s6}\varepsilon_6)+2b\,\sinh(z-\beta\delta_{16}\varepsilon_6),$$

$$D=\cosh(2z+\beta\delta_{s6}\varepsilon_6)+4b\,\cosh(z-\beta\delta_{16}\varepsilon_6)$$
$$+d+aa_6+a/a_6,$$

$$z=\frac{1}{2}\ln\frac{1+\eta}{1-\eta}+\beta\nu\eta-\beta\psi_6\varepsilon_6+\frac{\beta\mu_3E_3}{2},$$

$$a=\exp(-\beta\varepsilon),\quad b=\exp(-\beta w),$$

$$d=\exp(-\beta w_1),\quad a_6=\exp(-\beta\delta_{a6}\varepsilon_6).$$

The elastic, dielectric, and piezoelectric characteristics of the crystal will be calculated using the thermodynamic potential (Gibbs' function) $g_{1E}(T,\sigma_6,E_3,\eta)$

$$g_{1E}(T,\sigma_6,E_3,\eta)=\frac{\bar{v}}{2}c_{66}^{E0}\varepsilon_6^2-\bar{v}e_{36}^0\varepsilon_6E_3-\frac{\bar{v}}{2}\chi_{33}^0E_3^2+2T\ln 2$$
$$+2\nu\eta^2-2T\ln(1-\eta^2)$$
$$-2T\ln D-\bar{v}\sigma_6\varepsilon_6, \tag{6}$$

obtained from the electric thermodynamic potential $g_{2E}(T,\varepsilon_6,E_3,\eta)$

$$g_{2E}(T,\varepsilon_6,E_3,\eta)=U_{\text{seed}}+2T\ln \text{Sp}\exp(-\beta\hat{H}_q^{(4)})$$
$$-T\sum_{f=1}^{4}\ln \text{Sp}\exp(-\beta\hat{H}_{qf})$$
$$=g_{1E}(T,\sigma_6,E_3,\eta)+\bar{v}\sigma_6\varepsilon_6,$$

or the free energy $f(T,\varepsilon_6,P_3,\eta)$

$$f(T,\varepsilon_6,P_3,\eta)=g_{2E}(T,\varepsilon_6,E_3,\eta)-\bar{v}P_3E_3$$
$$=\frac{\bar{v}}{2}c_{66}^{P0}\varepsilon_6^2-\bar{v}h_{36}^0\varepsilon_6P_3$$
$$+\frac{\bar{v}}{2}\frac{1}{\chi_{33}^0}\left[P_3^2-\left(2\frac{\mu_3}{\bar{v}}\eta\right)^2\right]+2T\ln 2$$
$$+2\nu\eta^2-2T\ln(1-\eta^2)-2T\ln D, \tag{7}$$

where $h_{36}^0=e_{36}^0/\chi_{33}^0$, $c_{66}^{P0}=c_{66}^{E0}+e_{36}^0h_{36}^0$.

The thermodynamic equilibrium conditions

$$\frac{1}{v}\left(\frac{\partial g_{1E}}{\partial\varepsilon_6}\right)_{E_3,\sigma_6}=0,\quad \frac{1}{v}\left(\frac{\partial g_{1E}}{\partial E_3}\right)_{\sigma_6}=-P_3$$

or

$$\frac{1}{v}\left(\frac{\partial f}{\partial\varepsilon_6}\right)_{P_3}=\sigma_6,\quad \frac{1}{v}\left(\frac{\partial f}{\partial P_3}\right)_{\varepsilon_6}=E_3$$

yield

$$\sigma_6=c_{66}^{E0}\varepsilon_6-e_{36}^0E_3+\frac{4\psi_6}{\bar{v}}\frac{m}{D}+\frac{2M_6}{\bar{v}D}, \tag{8a}$$

$$P_3=e_{36}^0\varepsilon_6+\chi_{33}^0E_3+2\frac{\mu_3}{v}\frac{m}{D}, \tag{8b}$$

or

$$\sigma_6=c_{66}^{P0}\varepsilon_6-h_{36}^0\left(P_3-2\frac{\mu_3}{v}\frac{m}{D}\right)+\frac{4\psi_6}{\bar{v}}\frac{m}{D}+\frac{2M_6}{\bar{v}D}, \tag{9a}$$

$$E_3=-h_{36}^0\varepsilon_6+\frac{1}{\chi_{33}^0}\left(P_3-2\frac{\mu_3}{v}\frac{m}{D}\right), \tag{9b}$$

where

TABLE II. The theory parameters. The data in the second row taken from Ref. 13 were used in the theory where the spontaneous strain ε_6 was not taken into account.

ε	w	ν	ψ_6 (K)	δ_{s6}	δ_{a6}	δ_{16}	$c_{66}^{E0} \times 10^{-10}$ (dyn/cm^2)	$2\mu_3/v$ (μC/cm^2)	e_{36}^0 (esu/cm^2)	χ_{33}^0
91.3	795	34.13	-505	-680	1250	100	6.6	6.9	0.2×10^4	0.55
88.3	778	37.05								

$$M_6 = -\delta_{s6}\sinh(2z+\beta\delta_{s6}\varepsilon_6) + \delta_{a6}\left(aa_6 - \frac{a}{a_6}\right)$$
$$+ 4b\,\delta_{16}\sinh(z-\beta\delta_{16}\varepsilon_6).$$

Equations (8) and (9) can be approximated by familiar thermodynamic relations[8]

$$\sigma_6 = c_{66}^E\varepsilon_6 - e_{36}E_3,$$

$$P_3 = e_{36}\varepsilon_6 + \chi_{33}^\varepsilon E_3,$$

or

$$\sigma_6 = c_{66}^P\varepsilon_6 - h_{36}P_3,$$

$$E_3 = -h_{36}\varepsilon_6 + \frac{1}{\chi_{33}^\varepsilon}P_3,$$

where the elastic constant at constant field

$$c_{66}^E = \left(\frac{\partial\sigma_6}{\partial\varepsilon_6}\right)_{E_3}$$

$$= c_{66}^{E0} + \frac{8\beta\psi_6}{\bar{v}}\frac{-\varkappa\psi_6+r}{D-2\varkappa\varphi} + \frac{2\beta}{\bar{v}D^2}M_6^2$$

$$- \frac{2\beta}{\bar{v}D}\left[\delta_{s6}^2\cosh(2z+\beta\delta_{s6}\varepsilon_6) + \delta_{a6}^2\left(aa_6+\frac{a}{a_6}\right)\right.$$
$$\left. + 4b\,\delta_{16}^2\cosh(z-\beta\delta_{16}\varepsilon_6)\right] - \frac{4\varphi r^2}{\bar{v}TD(D-2\varkappa\varphi)},$$
$$\tag{10}$$

the coefficient of piezoelectric stress

$$e_{36} = \left(\frac{\partial P_3}{\partial\varepsilon_6}\right)_{E_3} = e_{36}^0 + \frac{2\mu_3}{v}\frac{\beta\theta}{D-2\varkappa\varphi},\tag{11}$$

and dielectric susceptibility of a clamped crystal (at ε_6 = const)

$$\chi_{33}^\varepsilon = \left(\frac{\partial P_3}{\partial E_3}\right)_{\varepsilon_6} = \chi_{33}^0 + \frac{\mu_3^2}{v}\frac{2\beta\varkappa}{D-2\varkappa\varphi}\tag{12}$$

are those characteristics of the crystal that have singularities at the transition point, whereas the constant of piezoelectric stress h_{36}

$$h_{36} = -\left(\frac{\partial E_3}{\partial\varepsilon_6}\right)_{P_3} = -\left(\frac{\partial\sigma_6}{\partial P_3}\right)_{\varepsilon_6} = \frac{e_{36}}{\chi_{33}^\varepsilon}\tag{13}$$

and the elastic constant c_{66}^P at constant polarization

$$c_{66}^P = \left(\frac{\partial\sigma_6}{\partial\varepsilon_6}\right)_{P_3} = c_{66}^E + e_{36}h_{36}\tag{14}$$

are the so-called "true" constants of the crystal. Here the following notations are used:

$$\varkappa = \cosh(2z+\beta\delta_{s6}\varepsilon_6) + b\cosh(z-\beta\delta_{16}\varepsilon_6) - \eta m,$$

$$r = \delta_{s6}\cosh(2z+\beta\delta_{s6}\varepsilon_6) - 2b\,\delta_{16}\cosh(z-\beta\delta_{16}\varepsilon_6) + \eta M_6,$$

$$\theta = -2\varkappa\psi_6 + r,$$

$$\varphi = \frac{1}{1-\eta^2} + \beta\nu.$$

Hence, having the microscopic expressions for c_{66}^E, e_{36}, and χ_{33}^ε, we can calculate other elastic, dielectric, and piezoelectric characteristics of the crystal: compliance at constant field

$$s_{66}^E = \left(\frac{\partial\varepsilon_6}{\partial\sigma_6}\right)_{E_3} = \frac{1}{c_{66}^E},\tag{15}$$

the coefficient of the piezoelectric strain

$$d_{36} = \left(\frac{\partial P_3}{\partial\sigma_6}\right)_{E_3} = e_{36}s_{66}^E,\tag{16}$$

the constant of piezoelectric strain

$$g_{36} = -\left(\frac{\partial E_3}{\partial\sigma_6}\right)_{P_3} = \frac{h_{36}}{c_{66}^P},\tag{17}$$

the dielectric susceptibility of a free crystal (at σ_6 = const)

$$\chi_{33}^\sigma = \left(\frac{\partial P_3}{\partial E_3}\right)_{\sigma_6} = \chi_{33}^\varepsilon + e_{36}d_{36}.\tag{18}$$

II. NUMERICAL RESULTS

A. The fitting procedure

In numerical calculations we shall consider a partially deuterated crystal with the transition temperature at ambient pressure $T_{C0} = 211.7$ K (a nominal deuteration $x=0.89$), hereafter abbreviated as KD$_2$PO$_4$. We also restrict ourselves to the effects of shear stress σ_6.

We need to set the values of the following theory parameters.

(a) The Slater energies ε, w, w_1, the so-called deformation potentials $\delta_{s6}, \delta_{a6}, \delta_{16}, \psi_6$, and the eigenvalue of the long-range interaction matrix Fourier transform ν (they determine the transition temperature as well as the dielectric, elastic, and piezoelectric characteristics associated with strain ε_6).

(b) The effective dipole moment μ_3 (it sets the magnitudes of dielectric and piezoelectric characteristics).

(c) The ``seed'' elastic constant c_{66}^{E0}, piezomodule e_{36}^0, and longitudinal dielectric susceptibility χ_{33}^0.

The adopted values of the theory parameters chosen as described below are presented in Table II. To determine them, we use the experimental data of Refs. 14,15 for the temperature dependences of the coefficient of piezoelectric strain d_{36}, dielectric susceptibility χ_{33}^σ, and compliance s_{66}^E of KD$_2$PO$_4$ at $\sigma_6 = 0$. Using Eqs. (10)–(18) and having the values of d_{36}, χ_{33}^σ, and s_{66}^E, we can find ``experimental'' points for the piezoelectric e_{36}, h_{36}, g_{36}, and elastic $c_{66}^P, c_{66}^E, s_{66}^P$, and dielectric susceptibility χ_{33}^ε.

We neglected contributions of double-ionized configurations, putting $w_1^0 \rightarrow \infty$. As the first approximation for the Slater energies ε and w and for the long-range interaction parameter ν, we use their values found earlier.[12,13] They provided a fair description of experimental data for the transition temperature, spontaneous polarization, dielectric permittivities, and specific heat of the crystal at ambient pressure within a theory where the shear strain ε_6 is not taken into account. The adopted in this paper values of ε and w are rather close to those of Refs. 12,13 (see Table II), whereas the value for the long-range interaction parameter is lower than the one used in the theories where spontaneous strain is not taken into account.[12]

The ε and ν are major parameters in setting the magnitude of the transition temperature, whereas w, effective dipole moment μ_3, piezoelectric parameter ψ_6 and splittings δ_{s6}, δ_{a6}, and δ_{16}, varied within physically reasonable limits, change T_{C0} only by a few degrees. The final values of the mentioned parameters were found such as to set the theoretical transition temperature at $\sigma_6 = 0$ to $T_{C0} = 211.7$ K and obtain the best description of the temperature curve of the compliance s_{66}^E and the piezomodule e_{36}, the magnitudes of h_{36} and g_{36} and their slopes $\partial h_{36}/\partial T$ and $\partial g_{36}/\partial T$ at $T > T_{C0}$, as well as the peak values and Curie constants of the permittivity ε_{33}^σ and the piezomodule d_{36}.

At the adopted values of ψ_6 and δ_{s6}, the magnitude of the piezoelectric field $-\psi_6 \varepsilon_6$ at spontaneous strain ε_6 taken just below the transition point is about 14% of the molecular field $\nu \eta$ created by dipole-dipole and lattice mediated interactions. Splitting of the up/down configuration energy $2\delta_{s6}\varepsilon_6$ is less essential and constitutes 7.5% of ε.

The value of c_{66}^{E0} was chosen by fitting the calculated $c_{66}^P(T)$ dependence to experimental data. The ``seed'' e_{36}^0 and χ_{33}^0 are merely the high temperature limits of experimental temperature dependences e_{36} and χ_{33}^ε, respectively.

B. Ambient pressure case

Figure 1 illustrates how the presented theory describes the temperature behavior of several related to the strain ε_6 elastic, piezoelectric, and dielectric characteristics of KD$_2$PO$_4$ at
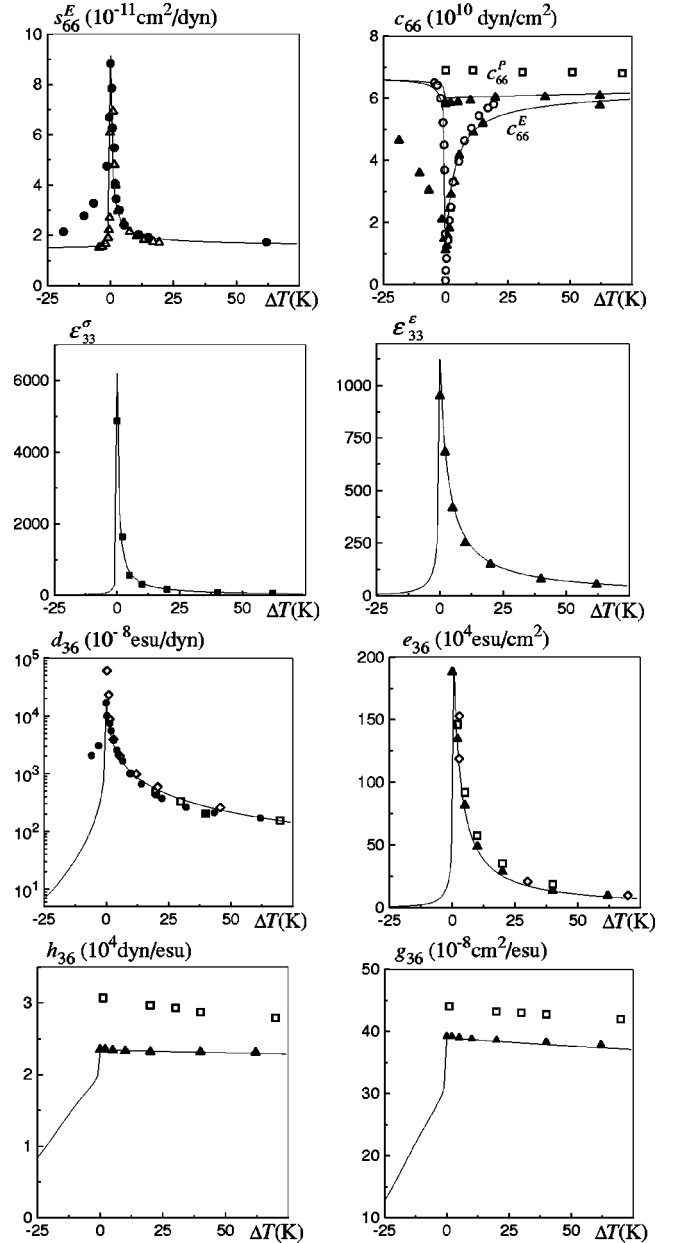

FIG. 1. Temperature dependences of the strain ε_6-related physical characteristics. Lines and solid symbols correspond to a deuterated KD$_2$PO$_4$; open symbols representing pure KH$_2$PO$_4$ are shown for comparison. Experimental points are taken from □: Ref. 16; ○: Ref. 17; ◇: Refs. 18,19; ■: Ref. 14; ●: Ref. 15; △ and ▲ are recalculated from Eqs. (10)–(18) using experimental data of Refs. 16,17 and Refs. 14,15, respectively.

atmospheric pressure. As one can see, the theoretical results are in a good quantitative agreement with the experimental data in the paraelectric phase. Apparent discrepancy between the theory and experiment in the ferroelectric phase can be related to a multi-domain structure of experimental samples, whereas the theory describes a single-domain ideal model.

The compliance s_{66}^E at $T \rightarrow T_{C0}$ has an anomalous increase; correspondingly, the elastic constant c_{66}^E nearly vanishes at the transition point. The elastic constant c_{66}^P at $T < T_{C0}$ is almost constant with temperature, has a small decrease at $T = T_{C0}$, and slightly increases in the paraelectric phase.
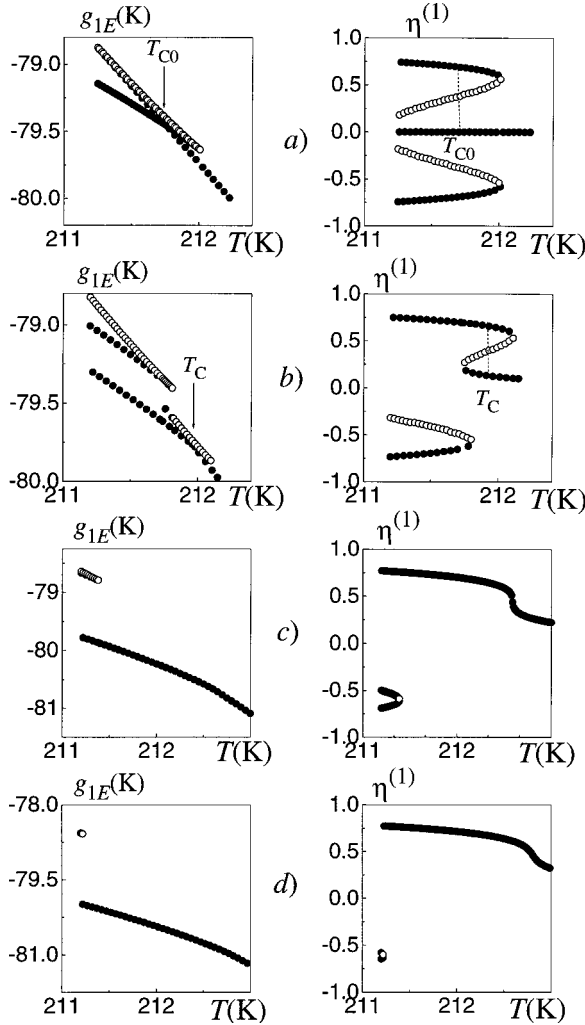
FIG. 2. Temperature dependences of the thermodynamic potential and solutions of equation for the order parameter at different values of stress σ_6: (a) $\sigma_6 = 0$, (b) $\sigma_6 < \sigma_6^*$, (c) $\sigma_6 = \sigma_6^*$, (d) $\sigma_6 > \sigma_6^*$. $\bigcirc$ and $\bullet$ correspond to maxima and minima of the thermodynamic potential, respectively.
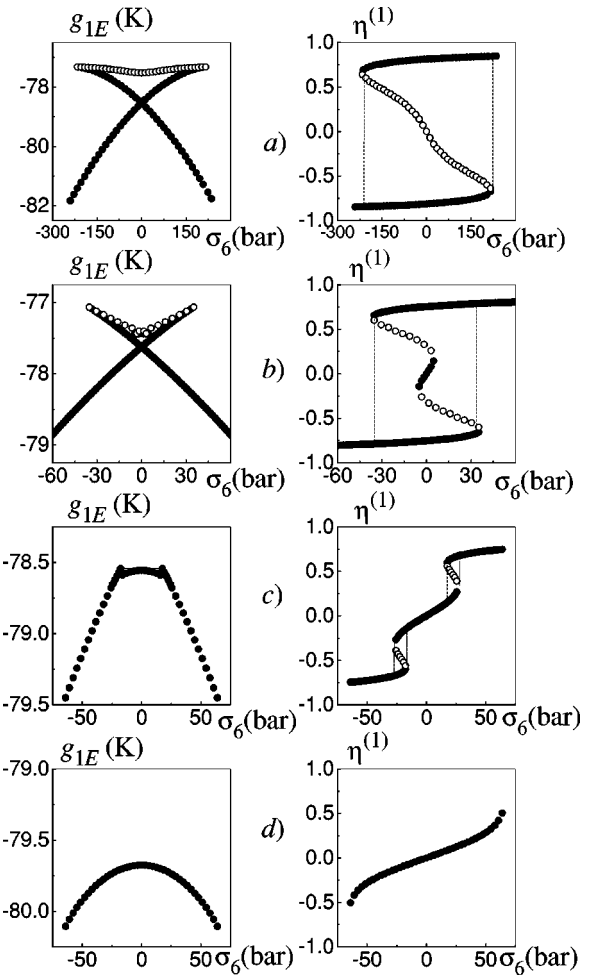

FIG. 3. Stress dependences of the thermodynamic potential and solutions of equation for the order parameter at different values of temperature: (a) $T \ll T_{C0}$, (b) $T < T_{C0}$, (c) $T_{C0} < T < T^*$, (d) $T^* > T$. $\bigcirc$ and $\bullet$ correspond to maxima and minima of the thermodynamic potential, respectively.

C. Nonzero σ_6 stress case

In Fig. 2 we plot the temperature dependences of the solutions of the equation for the thermodynamic potential g_{1E} extremum (5) and the corresponding values of g_{1E} at different values of stress σ_6 in the vicinity of the transition point. Equation (5) may have up to five different solutions, three of which correspond to minima, and two correspond to maxima of the thermodynamic potential. One of the minima—the
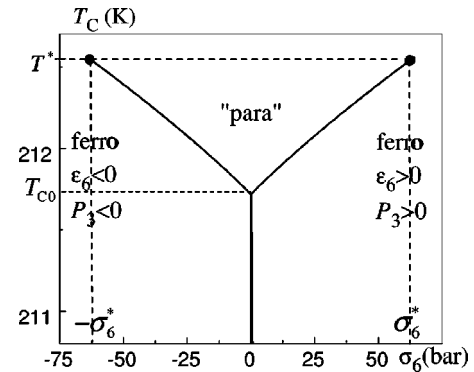
FIG. 4. T_C-σ_6 phase diagram of a KD$_2$PO$_4$ crystal.

Temperature dependences of the coefficient of piezoelectric strain d_{36}, coefficient of piezoelectric stress e_{36}, dielectric permittivities of a free (ε_{33}^σ) and clamped ($\varepsilon_{33}^\varepsilon$) crystals are similar. They all have singularities at the transition temperature, sharply increasing at $T \to T_{C0}$, with the increase in the ferroelectric phase being much faster than in the paraelectric phase. In contrast, the "true" piezoelectric constants of the crystal h_{36} and g_{36} do not exhibit singularities but have finite upward jumps at the ferroelectric transition and are almost independent of temperature above the transition point.

The presented graphs indicate that one can describe the temperature peculiarities of these dielectric, piezoelectric, and elastic properties of KD$_2$PO$_4$ attributing those peculiarities to deuteron subsystem only, with the heavy ions lattice counterpart considered as a temperature independent background. A dominating role in these peculiarities belongs to piezoelectric coupling, described by the parameter ψ_6, and to the short-range up-down deuteron configurations splitting, induced by strain ε_6 and described by the parameter δ_{s6}.
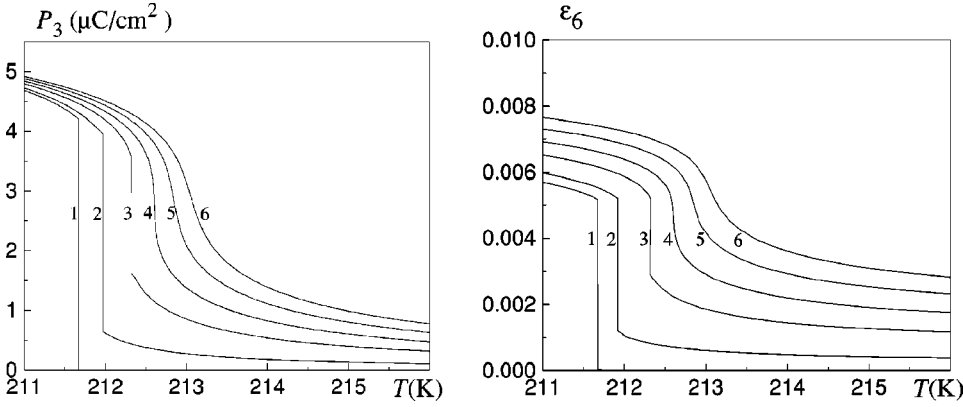
FIG. 5. Temperature dependences of polarization P_3 and strain ε_6 at different values of stress σ_6 (bar): 1–0; 2–15; 3–45; 4–$\sigma_6^* = 64$; 5–90; 6–110. Polarization was calculated with $2\mu_3/v = 6.2$ $\mu C/cm^2$.

central one—occurs at small values of the order parameter and has the same sign as that of the stress σ_6. The other two minima, if they exist, are nearly symmetric (exactly symmetric at $\sigma_6 = 0$), with the deeper minimum having the same sign as the stress.

Let $\eta_1 < 0$, $\eta_2 \approx 0$, and $\eta_3 > 0$ be the possible solutions of Eq. (5), corresponding to the minima of g_{1E}. As one can see (Fig. 2), at $\sigma_6 > 0$

$$g_{1E}(\eta_3) < g_{1E}(\eta_2) \quad \text{at} \quad T < T_C,$$

$$g_{1E}(\eta_3) = g_{1E}(\eta_2) \quad \text{at} \quad T = T_C \quad \text{(the transition criterion)},$$

$$g_{1E}(\eta_3) > g_{1E}(\eta_2) \quad \text{at} \quad T > T_C.$$

The temperature of the first order phase transition at which the branches of the thermodynamic potential $g_{1E}(\eta_3)$ and $g_{1E}(\eta_2)$ intersect increases with stress σ_6, and the value of η_2 at the transition point increases, whereas η_3 decreases. At a certain value of the stress σ_6^* the jump $\delta\eta$ becomes zero—there is a critical point where phase transition disappears. Further increase in the stress smears out the phase transition and results in a continuous and smooth temperature dependence of the order parameter. Such behavior is typical for the first order phase transitions in ferroelectrics in the electric field conjugate to the spontaneous polarization.[20]

The dependences of the values of the order parameter corresponding to the extrema of the thermodynamic potential on stress σ_6 at different temperatures in the vicinity of the transition point are depicted in Fig. 3. At $T < T_{C0}$, the branches of the thermodynamic potential $g_{1E}(\eta_1 < 0)$ and $g_{1E}(\eta_3 > 0)$ intersect, and the solutions of Eq. (5) η_1 and η_3 can exist simultaneously. Experimentally, on changing stress σ_6, a regular hysteresis loop $P_3 - \sigma_6$ should be observed. At $T_{C0} < T < T^*$, there can coexist only one of the nonzero minima and the central minimum of the thermodynamic potential (η_1 and η_2 or η_3 and η_2). Experiment should reveal a double hysteresis loop. At temperatures higher than the critical T^*, the dependences $g_{1E}(\sigma_6)$ and $\eta(\sigma_6)$ are smooth, and no jump in the order parameter is observed. Such a sequence of the hysteresis loops—a single loop at $T < T_{C0}$, a double loop at $T_{C0} < T < T^*$, and a gradual change at $T > T^*$—was obtained by Sidnenko and Gladkii[22] for KD$_2$PO$_4$ in the electric field E_3.

The corresponding $T_C - \sigma_6$ phase diagram of KD$_2$PO$_4$ is depicted in Fig. 4. Only the stable phases corresponding to absolute minima of thermodynamic potential are shown. The

following temperatures are indicated: $T_{C0} = 211.7$ K is the temperature of the first order phase transition at $\sigma_6 = 0$; $T^* = 212.6$ K is the temperature of the critical points at stresses $\pm\sigma_6^* = 64$ bar. The diagram is symmetric with respect to a change $\sigma_6 \rightarrow -\sigma_6$. An increase in the transition temperature with stress σ_6 is practically linear with the slope $\partial T_C/\partial|\sigma_6| = 13$ K/kbar.

The observed ''Y-shaped'' form of the phase diagram is not unique but typical for the systems in fields conjugate to the order parameter. The T_C-E phase diagram of the same topology was obtained within the phenomenological approach without invoking any microscopic model by Schmidt;[21] an increase in the transition temperature with E_3 and disappearance of the transition at certain critical E_3^* were observed experimentally[22] in KD$_2$PO$_4$ by examining the hysteresis loops.

In Fig. 5 we present temperature dependences of polarization P_3 and strain ε_6 at different values of stress σ_6. As one can see, these quantities exhibit similar variation with temperature and stress, and analogous are the corresponding experimental temperature curves of polarization at different fields E_3.[23] Spontaneous strain ε_6 and polarization P_3 slightly decrease with temperature and jump to zero at $T = T_{C0}$. Stress σ_6 induces nonzero ε_6 and P_3 above the transition temperature and increases their magnitudes below it. The jumps of ε_6 and P_3 at the transition point decrease with stress and vanish at σ_6^* and $T = T_C^*$. When the sign of the stress is reversed, the signs of strain and polarization reverse as well, but their absolute values do not change.

The major stress σ_6 effects on the physical characteristics are related to the changes induced by this stress in the character of the phase transition and, therefore, essential only in the vicinity of the transition point; at $|T - T_C| > 5$ K, these effects are negligibly small. Two examples of behavior of the physical characteristics with stress σ_6 are presented in Fig. 6. As σ_6 increases, the peak values of the quantities with anomalous temperature behavior (s_{66}^E, ε_{33}, d_{36}, and e_{36}) initially decrease. When σ_6 approaches the critical stress σ_6^*, they start to increase, and at $\sigma_6 = \sigma_6^*$ they are maximal. Further increase in stress σ_6 lowers the peaks and rounds up the cusps in the temperature curves of these characteristics.

Stress σ_6 effects on ''true'' characteristics of the crystal (c_{66}^P, h_{36}, and g_{36}) are analogous to those on polarization P_3 and strain ε_6: Up to σ_6^*, the stress reduces the jumps of these quantities at the transition point; at critical stress σ_6^*
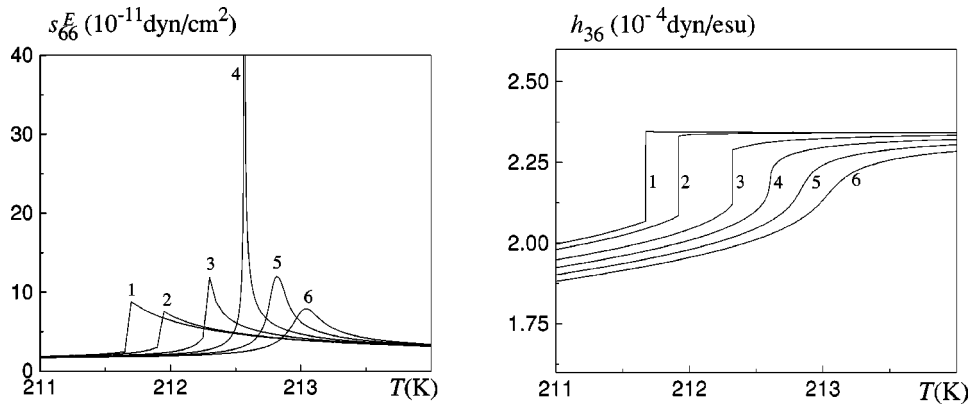
FIG. 6. Temperature dependences of the strain ε_6-related physical characteristics at different values of stress σ_6 (bar): 1–0; 2–15; 3–45; 4–$\sigma_6^*=64$; 5–90; 6–110.

the jumps vanish, and at $\sigma_6 > \sigma_6^*$ these quantities exhibit a gradual increase (h_{36} and g_{36}) or decrease ($c_{66}^P, P_3, \varepsilon_6$) with temperature.

III. CONCLUDING REMARKS

In this paper we presented the microscopic model for a description of stress σ_6 influence on the phase transition, static dielectric, elastic, and piezoelectric properties of deuterated ferroelectrics of the KD_2PO_4-type. Unlike hydrostatic or uniaxial $p = -\sigma_3$ pressures, the stress σ_6 lowers the symmetry of the high-temperature phase down to the symmetry of the low-temperature phase, inducing the strain ε_6 and, due to the piezoelectric effect, polarization P_3.

An important role in dependences of the transition temperature and dielectric characteristics of hydrogen bonded crystals of the KH_2PO_4 family on pressures that do not change the system symmetry is played by the corresponding changes in the D-site distance δ. Most likely, the stress σ_6 does not perceptibly affect δ. Instead, it distorts PO_4 groups and alters the angle between hydrogen bonds, perpendicular in an unstrained paraelectric crystal, thereby splitting the energies of deuteron configurations. Another important mechanism of the stress σ_6 influence on the phase transition and physical properties of the KD_2PO_4-type ferroelectrics is the piezoelectric coupling, which gives rise to the effective fields whose action, for the symmetry reasons, is equivalent to action of an external electric field applied along the ferroelectric axis. Taking into account the piezoelectric effect in the developed model allows one, at the proper choice of the

theory parameters, to describe quantitatively the available experimental data for the temperature dependences of dielectric, elastic, and piezoelectric characteristics of unstrained KD_2PO_4.

The transition temperature increases with the stress σ_6. Effects of stress σ_6 on the calculated dielectric, piezoelectric, and elastic characteristics are related to the changes in the character of the phase transition. In the constructed phase diagram, which is of the same topology as the $T_C - E$ diagram,[21,22] there are two symmetric critical points where the curves of phase equilibrium terminate, and the peak values of the physical characteristics of a crystal having peculiarities at the transition point are maximal. The stresses above critical smear out the phase transition and smoothen the temperature dependences of the characteristics.

Experimental verification of the obtained results for stress σ_6 influence on the phase transition and physical properties KD_2PO_4 type ferroelectrics appears to be difficult. In our next paper we shall present our calculations for the effects of the electric field E_3, the other field conjugate to the order parameter, which is more accessible to experimental verification.

*Email address: alla@icmp.lviv.ua

[1] G.A. Samara, Ferroelectrics **71**, 161 (1987).

[2] R.O. Piltz, M.I. McMahon, and R.J. Nelmes, Ferroelectrics **108**, 271 (1990).

[3] I.V. Stasyuk, R.R. Levitskii, and A.P. Moina, Phys. Rev. B **59**, 8530 (1999).

[4] R.J. Nelmes, Ferroelectrics **71**, 125 (1987).

[5] I.V. Stasyuk and I.N. Biletskii, Bull. Acad. Sci. USSR, Phys. Ser. **4**, 79 (1983).

[6] I. Smolyaninov and M.D. Glinchuk, J. Phys.: Condens. Matter **6**, 2869 (1994).

[7] R. Pirc, B. Tadic, and R. Blinc, Phys. Rev. B **36**, 8607 (1987).

[8] W. Kanzig, *Ferroelectrics and Antiferroelectrics* (Academic Press, New York, 1957).

[9] R. Blinc and S. Svetina, Phys. Rev. **147**, 430 (1966).

[10] R. Blinc and B. Žekš, *Soft Modes in Ferroelectrics and Antiferroelectrics* (Elsevier, New York, 1974).

[11] R. Blinc and B. Žekš, Helv. Phys. Acta **41**, 701 (1968).

[12] V.G. Vaks, N.E. Zein, and B.A. Strukov, Phys. Status Solidi A **30**, 801 (1975).

[13] R.R. Levitskii, I.R. Zachek, and Ye.V. Mits (unpublished).

[14] L.A. Shuvalov, I. S. Zheludev, A. V. Mnatsakanyan, Ts.-Zh. Ludupov, and I. Fiala, Izv. Akad. Nauk SSSR, Ser. Fiz. **31**, 1919 (1967).

[15] L.A. Shuvalov and A.V. Mnatsakanyan, Kristallografiya **11**, 222 (1966) [Sov. Phys. Crystallogr. **11**, 210 (1966)].

[16] W.P. Mason, Phys. Rev. **69**, 173 (1946).

[17] E.M. Brody and H.Z. Cummins, Phys. Rev. Lett. **21**, 1263 (1968).

[18] W. Bantle and C. Caflish, Helv. Phys. Acta **16**, 235 (1943).

[19] A. Von Arx and W. Bantle, Helv. Phys. Acta **16**, 211 (1943).

[20] A.F. Devonshire, Adv. Phys. **3**, 85 (1954).

[21] A. Western, A.G. Baker, C.P. Bacon, and V.H. Schmidt, Phys. Rev. B **17**, 4461 (1978).

[22] V.V. Gladkii and E.V. Sidnenko, Fiz. Tverd. Tela (Leningrad) **13**, 3092 (1971) [Sov. Phys. Solid State **13**, 2592 (1972)].

[23] E.V. Sidnenko and V.V. Gladkii, Kristallografiya **17**, 978 (1972) [Sov. Phys. Crystallogr. **17**, 861 (1973)].